JUDD OFELT ANALYSIS AND OPTICAL PROPERTIES OF Eu^{3+} DOPED TELLURITE GLASSES

TRAN THI HONG
Da Nang University of Education

PHAN TIEN DUNG
Institute of Materials Science, Vietnam Academy of Science and Technology

VU XUAN QUANG
Duy Tan University

E-mail: dungpt63@gmail.com

Abstract. *In this work, the structural characteristic and photoluminescence properties of Eu^{3+} doped B$_2$O$_3$-TeO$_2$ – ZnO-Na$_2$O glasses were investigated. These glasses were prepared by a melting method in air, combined with thermal annealing at 350 $^\circ$C, 450 $^\circ$C and 550 $^\circ$C for different duration times. The structural analysis results of these glasses revealed the formation of micro-crystals in the annealed host glass. The photoluminescence spectra of Eu^{3+} doped in these samples were observed. The local vibration mode around Eu^{3+} ions was investigated by the phonon side-band (PSB) associated with $^7F_0 - ^5D_2$ transition of Eu^{3+}. Judd-Ofelt parameters were then evaluated based on photoluminescence spectra and the luminescence intensity ratios of $^5D_0 \rightarrow ^7F_J$ (J = 2, 4 and 6) to $^5D_0 \rightarrow ^7F_1$ transition were predicted. The obtained results were then used to calculate Ω_2, Ω_4, Ω_6 parameters based on Judd-Ofelt theory. These Ω_2, Ω_4, Ω_6 parameters allow to derive radiative properties of Eu^{3+} ions in glass material such as transition probabilities, radiative lifetimes and peak stimulated emission cross-section for the $^5D_0 \rightarrow ^7F_J$ transitions.*

Keywords: Optical properties, luminescence, Judd-Ofelt theory, rare earth, Tellurite glasses .

I. INTRODUCTION

Oxide glasses are the most stable host matrices for practical applications due to their high chemical durability and thermal stability. Among the oxide glasses, tellurite glasses have proved to be interesting host for lanthanide ions, both from a fundamental and applied point of view. It is well known that the non-radiative loss is dominated by the highest energy phonon available in the matrix. Therefore, it is meaningful to select a host material that its maximum phonon energy is as low as possible. In silica, this phonon energy is reasonably large (about 1100 cm^{-1}). However, it is quite low for chalcogenide glasses (about 300 cm^{-1}), which lack many desirable features of silica-based glasses including mechanical strength and chemical durability. Tellurite glasses represent a compromise one among the desire for low phonon energy (650-750 cm^{-1}) [1–3] host

couple with the need to retain mechanical strength and process temperatures... However, less spectroscopic study on Borate-tellurite-zinc-sodium based glass was reported.

Among the Ln^{3+} ions used to optically activate the glass matrices, the trivalent europium ion Eu^{3+} ($4f^6$) is the mostly choice due to the fact that Eu^{3+} ($4f^6$) ions emit narrow band, almost monochromatic light, long lifetimes of optical active states. Eu^{3+} is also has been studied widely because of its simple electronic energy level scheme. Eu^{3+} ions exhibit pure magnetic and electric dipole transitions which are very sensitive probe for the rare earth ion site structure symmetry. The transition probability of hypersensitive transition ($^5D_o \rightarrow {}^7F_2$) of Eu^{3+} ion is depressed under higher symmetric environment whereas the magnetic dipole transitions are not affected by the environment. Their emission intensities are often used as internal standard [4, 5].

II. EXPERIMENTS

Using melting method, the $40B_2O_3.40TeO_2.10ZnO.10Na_2O$ glass containing Eu_2O_3 1 mol% concentration was prepared by two processes: melting followed by heated-treatment. B_2O_3, TeO_2, ZnO, Na_2CO_3 and Eu_2O_3 were used as starting materials. All components above were mixed by grinding them in a mortar gate carefully and dried at $100\,°C$ in the oven for 3h. The mixture was then melted at $1200\,°C$ in a Pt crucible in air for 2h. The fining step was carried out by keeping the melt at the temperature of $1150\,°C$ for 15min. After slowly cooling the melt down to room temperature, the transparent and colorless glass was obtained. Finally, obtained glass was annealed in oven at $350\,°C$ for 10h, $450\,°C$ for 15h and $550\,°C$ for 24h, respectively. Then was cut and polished for all optical measurements.

X–ray diffraction measurement was done on a XRD-D5000 SIEMENS diffractometer. Excitation and emission spectra of the samples were measured on a Horiba FluoroLog Spectrophotometer FL3-22 using a 450W xenon lamp source, monochromator (f/3.6 Czeny-Turner, double grating, all reflective optics) and R928P photomultiplier. Signals were recorded under computer control software FluorEssence 2.0 (powered by Origin 7.5). All the measurements were done at room temperature.

III. RESULTS AND DISCUSSION

III.1. Structural characterization

Generally, melting is a very strong method to fabricate glasses. Beside, heated-treatment for as-prepared glasses is also an important process because it makes structure of the glasses to be more stable. During this process, micro-crystals can be formed in the host glass which is called glass-ceramic materials.

XRD patterns of the glass samples are presented in Fig. 1. This figure shows the XRD patterns of the glass samples annealed at $350\,°C$ for 10 h (a), $450\,°C$ for 15 h (b) and $550\,°C$ for 24 h (c). The results of the structural analysis indicate that the glass sample annealed at $350\,°C$ for 10 h exhibits a pure amorphous phase, while the samples annealed at
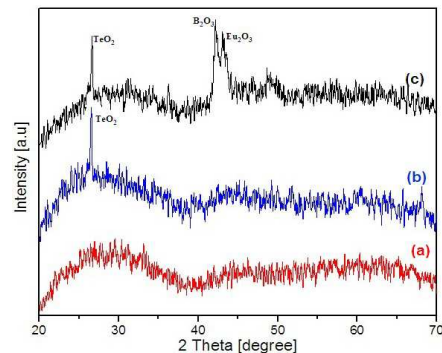

Fig. 1. XRD patterns of 1 mol % Eu^{3+} doped $40B_2O_3.40TeO_2.10ZnO.10Na_2O$ glass samples heated-treatment at $350\,°C$-10h (a), $450\,°C$-15h (b) and $550\,°C$-24h (c)

450 °C for 15 h and 550 °C for 24 h exhibit a mixture of amorphous and crystalline phases. It is known that the glass crystallization process is strongly dependent on the conditions of thermal annealing such as temperature, duration time and host components. Therefore, these preliminary results suggest the technological process preparing the glass-ceramic materials [6, 7].

III.2. Optimal properties

a. Excitation photoluminescence (PLE)

The excitation photoluminescence spectra for 612nm red emission of 1 mol% Eu^{3+} doped samples are shown in Fig. 2. The transitions of PLE were assigned (originating from $^7F_0$ and $^7F_1$) based on free-ion energy level structure and by taking into account both the electric and magnetic dipole contributions. There are fifteen obvious excitation peaks parking at 299nm, 304nm, 319nm, 327nm, 361nm, 365nm, 377nm, 382nm, 394nm, 400nm, 414nm, 465nm, 472nm, 526nm, 533nm. Among them, the intensity of 394nm excitation peak is greatest.

The PSB of the $^5D_2-^7F_0$ transition of the Eu^{3+} ion was observed in the excitation spectra shown in Fig.2. The PSB of the B$_2$O$_3$-base glass is attributed to the stretching vibration modes of B-O$^-$ and B-O of B$_2$O$_3$ and BO$_4^-$ units in tetra- and di-borate groups [8], where –O$^-$ and –O stand for the non-bridging oxygen (NBO) and bridging oxygen (BO), respectively. In fact, PSB is influenced both by the stretching vibration mode of NBO in the neighborhood of the Eu^{3+} ions and by the stretching vibration modes of NBO and BO which are apart from the Eu^{3+} ions.

The energy level diagram (Fig. 3) of Eu^{3+} shows the energy gaps among the levels of $^5G_2$, $^5L_6$, $^5D_3$, $^5D_2$, $^5D_1$ and $^5D_0$. The emission efficiencies of $^5D_3$, $^5D_2$ and $^5D_1$ levels are related to the non-radiative rate W_{NR} tightly. W_{NR} can be expressed by:

Fig. 2. Room temperature PLE (λ_{em}=612nm) of 1 mol% Eu^{3+} doped 40B$_2$O$_3$.40TeO$_2$.10ZnO.10Na$_2$O glass samples heated at 350 °C-10h (a), 450 °C-15h (b) and 550 °C-24h (c).
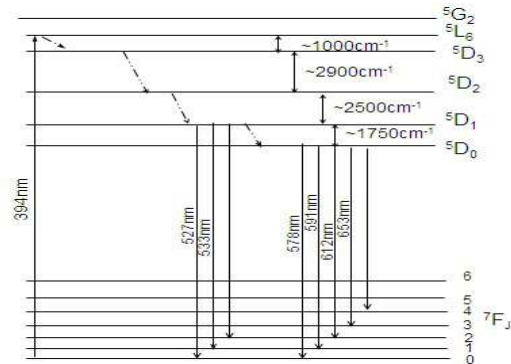
Fig. 3. Energy level diagram of Eu^{3+} in B$_2$O$_3$-TeO$_2$ –ZnO-Na$_2$O glasses

$$W_{NR} = W_P + W_{ET} \tag{1}$$

where W_P is the multiphonon decay rate and W_{ET} is the relaxation rate by energy transfer. For the lower concentration of Eu^{3+} doping, the contribution of W_{ET} can be ignored temporally, and the factor dominating the quantum efficiency is W_P, which is associated with the phonon energy, W_P
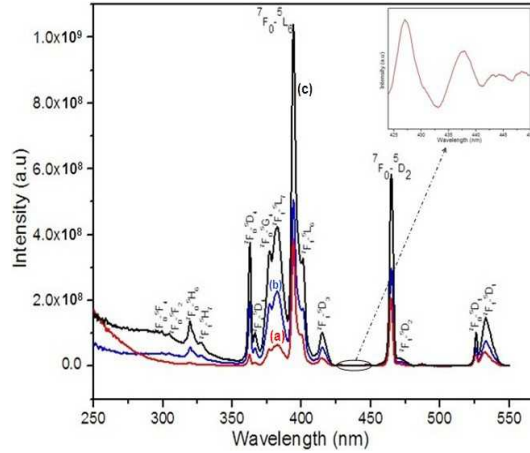
is expressed by:

$$W_P = W_0 \exp\left(\frac{-\alpha\Delta E}{\hbar\omega}\right) \qquad (2)$$

where ΔE is the optical energy gap to the next lower level and $\hbar\omega$ is the phonon energy of the glass and W_0 is the transition probability extrapolated to zero energy gap which is independent to the electronic nature of the RE ion. $\alpha = \ln[\Delta E/(\hbar\omega g)]$, where, g is the electron-phonon coupling strength [9]. According to Eq. (2), W_{NR} in silicate and phosphate should be much larger, with higher maximum-phonon energies ($\hbar\omega \sim 1100$ cm^{-1} and ~ 1300 cm^{-1}, respectively) than that in tellurite glass ($\hbar\omega \sim 750$ cm^{-1}). It is the main reason why the emissions of Eu^{3+} ions from $^5D_3$, $^5D_2$ and $^5D_1$ levels could not be observed in silicate and phosphate glasses but can be recorded in tellurite (40B$_2$O$_3$.40TeO$_2$. 10ZnO.10Na$_2$O.1Eu^{3+}) glasses clearly.

b. Photoluminescence (PL)

Fig. 4 shows the photoluminescence spectra of 1 mol% Eu^{3+} doped samples. These spectra were obtained by exciting the $^5L_6$ state using the 394 nm wavelength of a broad band xenon lamp source. Emissions are mainly observed for $^5D_0 \rightarrow ^7F_J$(J=0, 1, 2, 3, 4) transitions (with maximums at 578 nm; 591 nm; 612 nm; 653 nm and 700 nm, respectively) and a few weak emissions are noticed for $^5D_1 \rightarrow ^7F_{0,1,2}$ (with the maximums at 527 nm; 534 nm; 553 nm, respectively) which are assigned in Fig. 4. It can be seen obviously that increasing the temperature of the heated- treatment process leads to the intensity increase of the spectrum significantly.

The emission intensities of $^5D_0 \rightarrow ^7F_{2,4}$ transitions are induced electric dipole allowed and depend strongly on the local symmetry

Fig. 4. Rom temperature PL (λ_{ex} = 394 nm) of 1 mol% Eu^{3+} doped 40B$_2$O$_3$.40TeO$_2$.10ZnO.10Na$_2$O glass samples heat-treatment 350 °C-10h(a), 450 °C-15h(b) and 550 °C-24h (c)

around Eu^{3+} ions. Moreover, the $^5D_0 \rightarrow ^7F_2$ is said to be hypersensitive transition (under the selection rule ΔJ =2) to the surrounding environment, whereas the transition $^5D_0 \rightarrow ^7F_1$ is magnetic dipole allowed and independent of the local symmetry.

Therefore, the ratio of integrated emission intensity of the $^5D_0 \rightarrow ^7F_2$ transition to that of the $^5D_0 \rightarrow ^7F_1$ transition, defined as fluorescence intensity ratio R, is the spectroscopic key to estimate the deviation from the site symmetry of the Eu^{3+} ions. Sometime, R is also defined as asymmetry ratio. In our experiments, the emission spectra were recorded for the sample 40B$_2$O$_3$.40TeO$_2$.10ZnO.10Na$_2$O.1Eu$_2$O$_3$ excited by the wavelength of 394nm. The fluorescence intensity ratio R were found to be 4.1; 3.9 and 3.8 corresponding to the glass samples heated-treatment at 350 °C-10 h; 450 °C-15h and 550 °C-24 h, respectively. According to Kumar *et al.* [10], most of the Eu^{3+} doped glasses exhibit the *R* values in the range of 3.5-4.2. This indicates the potential of Borate-tellurite-zinc-sodium: Eu^{3+} glass as a promising laser and red luminescence material.
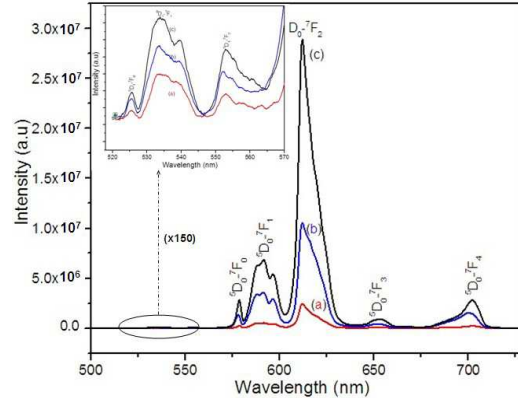
III.3. Judd- Ofelt analysis

The Judd-Ofelt theory was often used to calculate the intensity parameters Ω_λ (λ=2, 4, 6). The intensity parameters Ω_λ could be obtained from absorption spectra. But sometimes, it is very difficult to measure absorption spectra. However, the strong luminescence is a characteristic feature of many europium doped materials [11]. Therefore, the Judd-Ofelt (J-O) analysis by emission spectra is frequently used for the Eu^{3+} doped host matrices.

The emission spectra of Borate-tellurite-zinc-sodium: Eu^{3+} ion excited by 394 nm light are shown in Fig.4. Among them, three main emission peaks $^5D_0 \rightarrow ^7F_1$; $^5D_0 \rightarrow ^7F_2$ and $^5D_0 \rightarrow ^7F_4$ were used to calculate the J-O parameters.

The $^5D_0 \rightarrow ^7F_1$ is the magnetic dipole transition and its spontaneous emission probability A_{md} is given by the following expression [4, 5]:

$$A_{md} = \frac{64\pi^4}{3h} \frac{v^3}{2J+1} n^3 S_{md} \tag{3}$$

where v is the wavenumber of transition, h is the Planck constant, J is the total angle momentum of the excited state, n is the refractive index and S_{md} is the magnetic-dipole line strength which is a constant and independent of the host material.

The A_{md} can be estimated by using the reference value of A'_{md} published somewhere and the relationship $A_{md} = (n/n')^3 A'_{md}$; where A'_{md} and n' are the spontaneous emission probability and refractive index of the reference material, respectively. For example, in the case of lithium fluoroborate glasses doped with 1 mol % Eu^{3+}, $A'_{md} = 51.9$ s^{-1} and $n' = 1.539$ [12].

The $^5D_0 \rightarrow ^7 F_{J=2,4,6}$ transitions are electronic dipole allowed. The spontaneous emission probability A_{ed} of electronic transition is given by:

$$A_{ed} = \frac{64\pi^4 e}{3h} \frac{v_J^3}{2J+1} \frac{n(n^2+2)^2}{9} S_{ed} \tag{4}$$

where v_J is the wavenumber of transition $^5D_0 \rightarrow ^7 F_J$; e is the electron charge; h is the Planck constant; n is the refractive index; J is the total angle momentum of excited state and S_{ed} is the electric-dipole line strength of the transition [13].

The emission intensity I of a given transition is proportional to the area S under the emission curve: $I = hvA_r N\alpha S$. Where hv is the transition energy, A_r is the radioactive transition rate and N is the population of emitting level ($^5D_0$). Thus, Ω_λ parameters could be evaluated simply by the ratio of the intensity of the $^5D_0 \rightarrow ^7 F_{J=2,4,6}$ transitions to the intensity of $^5D_0 \rightarrow ^7 F_1$ transition:

$$\frac{\int I_J dv}{\int I_1 dv} = \frac{A_J}{A_1} = \frac{e^2}{S_{md1}} \frac{v_J^3}{v_1^3} \frac{n(n^2+2)^2}{9n^3} \Omega_J \left\| U^J \right\|^2 \tag{5}$$

where $\left\| U^J \right\|^2 \equiv (\Psi J \left\| U^J \right\| \Psi' J')^2$ is the square of the matrix elements of the tensor operator, which connects $(\Psi J|$ to final state $|\Psi' J')$ and is considered to be independent of host matrix. The value of for every transition of the RE^{3+} ions could be found in the published tables [12, 13]. As seen from Eq. (5), Ω_2 and Ω_4 can be evaluated independently from the emission transitions of $^5D_0 \rightarrow ^7 F_2$ and $^5D_0 \rightarrow ^7 F_4$. But, Ω_6 cannot be evaluated because of limitation of our experimental conditions. Since the emission transition $^5D_0 \rightarrow ^7 F_6$ at about 810nm has not been observed from the emission spectra, Ω_6 parameter could not be determined in our experiment because the $^5D_0 \rightarrow ^7 F_6$ emission

intensity is usually very weak compared to intensities of the $^5D_0 \to^7 F_2$ and $^5D_0 \to^7 F_4$ transitions. The calculated Ω_2 and Ω_4 parameters are presented in Table 1.

Table 1. Judd-Ofelt parameters ($\Omega_\lambda \times 10^{-20}$ cm^2)

Ω_λ	The sample (350°-10 h)	The sample (450°C-15 h)	The sample (550°C-24 h)
Ω_2	4.872	4.718	4.614
Ω_4	1.463	1.487	1.519
Ω_6	——	——-	——-

From Table 1, the Ω_2 value is greater than Ω_4 and the value of Ω_6 cannot be evaluated in every samples. Thus, it can be concluded that the radiative transition probabilities are mainly dependent on the $^5D_0 \to^7 F_2$ red hypersensitive emission transition. This result is in agreement with that of the other tellurite glasses [14].

According to Ref. [15, 16], the fluorescence intensity ratio R of $^5D_0 \to^7 F_2$ to $^5D_0 \to^7 F_1$ transition was used to establish the degree of asymmetry in the vicinity of Eu^{3+} ions and Eu-O covalent. Moreover, the R value also depends on the J-O parameter Ω_2, which was used to explain the short-range effects. Therefore, change of R, and in turn, Ω_2 give information about the short range effect on local structure around Eu^{3+} ions and Eu-O covalent. The higher value of R, the lower symmetry around the Eu^{3+} ions and the higher the Eu-O covalent. It also can be seen from Table 1 that increase of the heat-treated temperature leads to the significantly decrease of R and Ω_2, but Ω_4 increase. It can be explained that when the heat-treated temperature increases, the degree of symmetry in the vicinity of Eu^{3+} ions increases and so does the rigidity.

The Judd-Ofelt theory parameters not only can give the information on local structure and binding state of RE –ions in host matrices, but also from the parameters Ω_λ, several important optical properties such as branching ratio, relative transition probabilities, lifetimes of the excited states… could be evaluated. The radiative transition probability for transition $\psi J \to \psi' J'$ is given by:

$$A(\psi J \to \psi' J') = A_{ed} + A_{md}$$

The calculated radiative life time τ_{cal} of the excited state can be obtained from A_{total} : $A_{total}(\psi J) = \sum_{\psi' J'} A(\psi J, \psi' J') = 1/\tau_{cal}$. So in order to receive τ_{cal} of $^5D_0$ state, it is necessary to evaluate the radiative transition probabilities of the $^5D_0 \to^7 F_1$, $^5D_0 \to^7 F_2$ and $^5D_0 \to^7 F_4$ transitions. Because the reduced matrix is small, the $^5D_0 \to^7 F_6$ transition is also negligible, so the A_{ed} of this transition can be negligible in τ_{cal}. The branching ratio is given by $\beta_R(\psi J, \psi' J') = A(\psi J, \psi' J')/A_{total}(\psi J)$.

Table 2. The branching ratio $\beta_R(^5D_0 \to^7 F_2)(\%)$, the life time of the excited τ_{cal} and τ_{exp} of samples.

(350°C-10 h)	The sample (450°C-15 h)	The sample (550°C-24 h)	The sample
τ_{cal}(ms)	2.984	3.118	3.269
τ_{exp}(ms)	1.181	1.235	1.244
$\beta_R(^5D_0 \to^7 F_2)(\%)$	72.56	73.32	75.14

From Table 2, the calculated lifetime τ_{cal} of the excited state ($^5D_0$) of this Borate-tellurite-zinc-sodium is longer than the experimental lifetime τ_{exp}. This is perfectly reasonable. The experimental life time (τ_{exp}) is always contributed from both of conversions: emission and non-emission. Meanwhile, the life time (τ_{cal}) is only contributed from emission.

IV. CONCLUSION

1 mol% Eu^{3+}- doped $40B_2O_3.40TeO_2.10ZnO.10Na_2O$ glasses were studied. In the case of samples heated at 450 °C for 15 h and 550 °C for 24 h, the crystalline formation is dominated. These results revealed that 450 °C and 15 h are the temperature and duration time, needed to form crystalline phases in the Borate-tellurite-zinc-sodium glass. The PSB of the $^5D_2 - ^7F_0$ transition of Eu^{3+} ions was evaluated from the excitation spectrum. Emission spectra were then used to calculate Ω_2, Ω_4 parameters based on Judd-Ofelt theory. Obtained results of the Ω_2, Ω_4 parameters revealed that the radiative transition probabilities depend mainly on the $^5D_0 \rightarrow ^7F_2$ red hypersensitive emission transition. A relatively higher Ω_2 value of the sample heated at 350 °C for 10 h compared to the samples heated at 450 °C for 15 h and 550 °C for 24 h could be due to the higher asymmetry around Eu^{3+} ions in this non-linear optical material. The high brightness and short lifetime of $^5D_0 \rightarrow ^7F_2$ emission show the good potential application of Borate-tellurite-zinc-sodium glass in photonics.

ACKNOWLEDGMENT

REFERENCES

[1] A. Hishikawa, H. Hasegawa, and K. Yamanouchi, *J. Electron Spectrosc. Relat. Phenom.* **141** (2004) 195-200.

[2] C. Joshi, R. N. Rai, and S. B. Rai, *Journal of Quantitative Spectroscopy & Radiative Transfer* **113** (2012) 397-404.

[3] M. Clara Goncalves, Luis F. Santos, and Rui M. Almeida, *Rare Earth-doped Transparent Glass Ceramic. C.R. Chimie* **5** (2002) 845-854

[4] G. S. Ofelt, *J. of Chemical Physics* **17**(3) (1962) 511-520.

[5] B. R. Judd, *Physical Review* **127**(3) (1962) 750-761.

[6] G. Lakshminarayana and Jianrong Qiu, *Journal of Alloys and Compounds*, **476**(1-2) (2009) 720727.

[7] Daliang Zhao, Xvsheng Quiao, Xianping Fan, and Minquan Wang,

[8] S. Tanabe, S. Todoroki, K. Hirao, N. Soga, *J. Non-Cryst. Solids* **122**(1)(1990) 59.

[9] T. Miyakawa, D.L.Dexter, *Phys.Rev. B* **1**(7) (1970) 2961-2969.

[10] A. Kumar, D. K. Rai, S. B. Rai, *Spectrochimica Acta Part A* **58** (2002) 2115-2125.

[11] K. Binnemans, *Bull. Soc. Chim. Belg.* **105**(12) (1996) 793-798.

[12] P. Babu, C. K. Jayasankar, *Physics B* **279** (2000) 262-281.

[13] W. T. Carnall, P. R. Fields, and K. Rainak, *J. of Chemical Physics* **49**(10) (1968) 4450-4455.

[14] R. Arifin and M. Rahim Bin Sahar, *Solid State Science and Technology* **10**(1) (2008) 29-36.

[15] C. Goerller-Walrand, K. Binnemans, *Handbook on Physics and Chemistry of Rare Earth*, Chapter 167, Spectral Intensities of f-f Transitions, pp. 101-264, 1998.

[16] R. Reisfeld, *Structure Bonding* **22** (1975) 123-175.